International Journal of Nanoscience
Vol. 10, No. 3 (2011) 447–453

DOI: 10.1142/S0219581X11008216

NONLINEAR VIBRATION AND BENDING INSTABILITY OF A SINGLE-WALLED CARBON NANOTUBE USING NONLOCAL ELASTIC BEAM THEORY

I. MEHDIPOUR[*], P. SOLTANI[*,‡,§], D. D. GANJI[†]
and A. FARSHIDIANFAR[‡]

[*]*Department of Mechanical Engineering*
Semnan Branch, Islamic Azad University
Semnan, Iran

[†]*Department of Mechanical Engineering*
Babol University of Technology, Babol, Iran

[‡]*Department of Mechanical Engineering*
Ferdowsi University of Mashhad
Mashhad, Iran

[§]*p.soltani@semnaniau.ac.ir*
[§]*payam.soltani@gmail.com*

Received 20 February 2010
Accepted 30 October 2010

Due to the nonlocal Euler–Bernoulli elastic beam theory, the effects of rippling deformation on the bending modulus and the structural bending instability of a single-walled carbon nanotube (SWCNT) are investigated. The nonlinear vibrational model of a cantilevered SWCNT is solved using the perturbation method of multiscales. The nonlinear resonant frequency and the associated effective bending modulus of the carbon nanotube (CNT) are derived analytically. The effects of the nonlocal parameter, the external harmonic force, and the diameter-to-length ratio on the effective bending modulus are discussed widely. Moreover, the model can predict special kind of structural instability due to the rippling deformation called rippling instability. The results show that the nonlocal theory forecasts larger values for the effective bending modulus compared with the classical beam theory, especially for the stubby CNTs. Meanwhile, the rippling instability threshold will move to the higher values of the diameter-to-length ratio based on the nonlocal beam theory comparing with the local ones.

Keywords: Carbon nanotubes; nonlinear vibration; rippling deformation; bending instability.

1. Introduction

Since their initial discovery by Iijima (1991), carbon nanotubes (CNTs) have come under ever-increasing scientific scrutiny because they possess excellent mechanical properties, such as extremely high strength, stiffness, and resilience. These, together with other distinctive physical properties, result in many prospective applications, such as strong,

[§]Corresponding author.

light and high toughness fibers for nanocomposite structures, parts of nanodevices, hydrogen storage, micromechanical oscillators, etc.[1–5] The most individual mechanical property of CNTs is high stiffness and high Young's modulus. There are several studies to predict Young's modulus of CNTs experimentally. Treacy *et al.*[6] obtained Young's modulus of 1.8 TPa (as an average value) for multiwalled nanotubes, while Krishnan *et al.*[7] obtained it for about $1.25 - 0.35/{+0.45}$ TPa for single-walled nanotubes (SWCNTs). Young's modulus of 1.28 ± 0.5 TPa also has been calculated for multiwalled carbon nanotubes by Wong *et al.*[8] experimentally. In all previous researches, Young's modulus of CNTs has been predicted to be more than 1 Tpa, but, when CNTs are under bending deformation and pursuant to high flexibility of CNTs, the rippling configuration of the SWCNT affects the stiffness of CNTs directly and effectively. Poncharal *et al.*[9] measured Young's modulus E of a multiwalled carbon nanotubes and found the calculated E decreasing from about 1 to 0.1 TPa with the diameter D increasing from 8 to 40 nm. They showed that the appearance of rippling deformation in bending mode of CNTs caused the stiffness to decrease dramatically, thus, the linear elastic theory will not predict the mechanical behavior of CNTs with rippling deformation. A finite element approach has been used to estimate the nonlinear relationship between the bending moment against the curvature of a bent SWCNT with rippling deformation[10,11] and the effective elastic modulus has been calculated using nonlinear analysis due to the local elastic Euler–Bernoulli beam theory.

In the present study, the nonlocal Euler–Bernoulli beam theory is applied to investigate the effective resonant frequency and the corresponding bending modulus of a cantilevered SWCNT with rippling deformation. Moreover, the nonlinear model can predict the structural instability of CNTs with rippling deformation for bending mode, which is called the rippling instability. The effects of the nonlocal parameter, the excitation load-to-damping ratio, and the diameter-to-length ratio on the nonlinear frequency, the effective bending modulus of the SWCNT, and the rippling instability threshold are widely discussed.

2. Nonlocal Elastic Beam Theory

The governing equation of motion for forced vibration of a SWCNT with the nonlocal Euler–Bernoulli beam theory can be expressed[12] as

$$\begin{aligned} M''(x,t) &+ 2\mu\dot{w}(x,t) \\ &+ \rho A\frac{\partial^2}{\partial t^2}\left[w(x,t) - (e_0a)^2\frac{M(x,t)}{EI}\right] \\ &= F(x,t)\,, \end{aligned} \tag{1a}$$

$$F(x,t) = G(x)\cos(\tilde{\omega}t)\,, \tag{1b}$$

where $M(x,t)$ denotes the bending moment, $w(x,t)$ denotes the beam deflection function, ρ is mass density, EI is bending rigidity, A is cross-sectional area of SWCNT, and μ is the damping coefficient. e_0a is a nonlocal parameter revealing the nanoscale effect on the response of structures,[12–14] $F(x,t)$ is the excitation load measured per unit length exerted from an electrical harmonic field, and $w'(x,t)$ and $\dot{w}(x,t)$ are the partial derivatives $\partial w(x,t)/\partial x$ and $\partial w(x,t)/\partial t$, respectively. The corresponding boundary condition for a cantilevered beam is expressed as

$$\begin{aligned} w(0,t) &= w'(0,t) = 0\,, \\ w''(L,t) &= w'''(L,t) = 0\,, \end{aligned} \tag{2}$$

where L is the length of the SWCNT.

2.1. *Nonlinear vibration model*

As a CNT bends, the rippling deformation occurs specially for the relatively and locally large deformations.[10] In this case, the linear relationship between the bending moment and the curvature of the CNT does not match anymore. The nonlinear relation between the bending moment M and the curvature κ has been estimated as a ninth order polynomial equation for the rippling deformation as follows[11]:

$$\begin{aligned} M(x,t) = EI\kappa(1 &- a_3D^2\kappa^2 + a_5D^4\kappa^4 \\ &- a_7D^6\kappa^6 + a_9D^8\kappa^8)\,, \end{aligned} \tag{3}$$

where D is the diameter of CNT, $a_3 = 1.755 \times 10^3$, $a_5 = 2.0122 \times 10^6$, $a_7 = 1.115 \times 10^9$, and $a_9 = 2.266 \times 10^{11}$.

And the second partial derivative of Eq. (3) with respect to x is

$$\begin{aligned} M''(x,t) = EI[\kappa''(1 &- 3a_3D^2\kappa^2 + 5a_5D^4\kappa^4 \\ &- 7a_7D^6\kappa^6 + 9a_9D^8\kappa^8) \\ &+ (\kappa')^2(-6a_3D^2\kappa + 20a_5D^4\kappa^3 \\ &- 42a_7D^6\kappa^5 - 72a_9D^8\kappa^7)]\,. \end{aligned} \tag{4}$$

For large deflection, the relation between the bending curvature $\kappa(x,t)$ against the beam deflection $w(x,t)$ can be expressed as

$$\begin{aligned}\kappa(x,t) &= \frac{w''(x,t)}{[1+w'(x,t)^2]^{3/2}} \\ &= w''\left[1-\frac{3}{2}(w')^2+\frac{15}{8}(w')^4-\cdots\right] \\ &\cong w''(x,t)[1-r(w')^2]\,, \end{aligned} \tag{5}$$

where $r = 1.5$.

Substituting Eq. (5) into Eqs. (3) and (4), yields

$$M(x,t) = EI\{w'' - 3a_3D^2w''^3 - rw'^2w''\} \tag{6}$$

and

$$\begin{aligned}M''(x,t) = EI\{w'''' &- 3a_3D^2[2w''(w''')^2 + (w'')^2w''''] \\ &- r[2(w'')^3 + 6w'w''w''' + (w')^2w'''']\}\,.\end{aligned} \tag{7}$$

The nonlinear vibrational equation will be obtained by substituting Eqs. (6) and (7) into Eq. (1):

$$\begin{aligned}&EIw'''' + 2\mu\dot{w} + \rho A\frac{\partial^2}{\partial t^2}\{w(x,t) \\ &\quad - (e_0a)^2[w'' - 3a_3D^2w''^3 - rw'^2w'']\} \\ &\quad = EIN(w) + F(x,t)\,,\end{aligned} \tag{8a}$$

where $N(w)$ is

$$\begin{aligned}N(w) = &\,3a_3D^2[2w''(w''')^2 + (w'')^2w''''] \\ &+ r[2(w'')^3 + 6w'w''w''' + (w')^2w'''']\,.\end{aligned} \tag{8b}$$

Making all the variables in Eqs. (8) dimensionless by using the characteristic length L, time $L^2\sqrt{\rho A/EI}$ and force EI/L^3 give

$$\begin{aligned}&\bar{w}'''' + 2\bar{\mu}\dot{\bar{w}} + \ddot{\bar{w}} - (e_n)^2\frac{\partial^2}{\partial t^2} \\ &\quad \times\left(\bar{w}'' - 3a_3\left(\frac{D}{L}\right)^2\bar{w}''^3 - r\bar{w}'^2\bar{w}''\right) \\ &\quad = \bar{N} + \bar{F}(x^*,t^*),\end{aligned} \tag{9a}$$

$$\bar{F}(x^*,t^*) = \bar{G}(x^*)\cos(\tilde{\omega}^*t^*)\,, \tag{9b}$$

where

$$\begin{aligned}&x^* = x/L\,, \quad t^* = t\sqrt{EI/\rho A}/L^2\,, \quad \bar{w} = w/L\,, \\ &e_n = e_0a/L\,, \quad \bar{\mu} = \mu L^2/\sqrt{EI\rho A}\,, \\ &\bar{N} = N/L^3\,, \quad \bar{G} = GL^3/EI\,.\end{aligned} \tag{10}$$

The associated dimensionless boundary condition in Eq. (2) is

$$\begin{aligned}\bar{w}(0,t^*) &= \bar{w}'(0,t^*) = 0\,, \\ \bar{w}''(1,t^*) &= \bar{w}'''(1,t^*) = 0\,.\end{aligned} \tag{11}$$

2.2. *Nonlinear analysis*

The perturbation method of multiscales[15] has been applied to calculate the resonant frequency $\tilde{\omega}$ for a SWCNT with rippling deformation. The beam deflection w can be expanded using small perturbation parameter ε into $w = u_0 + \varepsilon u$, where u_0 should be zero. To make the exciting and the damping forces both be of the same orders as the nonlinear terms, the parameters $\bar{\mu} = \varepsilon^2 \upsilon$ and $\bar{G}(x^*) = \varepsilon^3 g(x^*A)$ are determined[15] and Eq. (9) will be

$$\begin{aligned}&u'''' + 2\varepsilon^2\upsilon\dot{u} + \ddot{u} - (e_n)^2\frac{\partial^2}{\partial t^2} \\ &\quad \times\left[u'' - 3a_3\left(\frac{D}{L}\right)^2u''^3 - ru'^2u''\right] \\ &\quad = \varepsilon^2N_u + \varepsilon^2g\cos(\tilde{\omega}^*t^*)\,,\end{aligned} \tag{12a}$$

where

$$\begin{aligned}N_u = &\,3a_3(D/L)^2[2u''(u''')^2 + (u'')^2u''''] \\ &+ r[2(u'')^3 + 6u'u''u''' + (u')^2u'''']\,.\end{aligned} \tag{12b}$$

In the previous equations, $u(x^*,t^*)$ and $g(x^*)$ are, respectively, expanded as

$$\begin{aligned}u(x^*,t^*) &= \sum_{n=1}^{\infty} q_n(t^*)\phi_n(x^*)\,, \\ g(x^*) &= \sum_{n=1}^{\infty} g_n\phi_n(x^*)\,,\end{aligned} \tag{13}$$

where $q_n(t^*)$ shows the dynamic response of SWCNT, g_n is the amplitude of the exciting force, and ϕ_n for $n = 1, 2, 3, \ldots$ represent the normalized mode functions of the beam from the linear vibration analysis due to the specified boundary condition. Meanwhile, the mode function ϕ_n satisfies the following formula:

$$\begin{aligned}&\int_0^1 \phi_i(x^*)\phi_j(x^*)dx^* = 0 \quad (i \neq j)\,, \\ &\int_0^1 \phi_i(x^*)\phi_j(x^*)dx^* = 1 \quad (i = j)\,.\end{aligned} \tag{14}$$

Substituting Eq. (13) into Eqs. (12) and utilizing Eqs. (14), we have

$$\begin{aligned}(1-\lambda e_n^2)\ddot{q}_1 + 2\varepsilon^2 \upsilon \dot{q}_1 + \omega_1^2 q_1 \\ + e_n^2 \alpha_1 \varepsilon^2 (3\ddot{q}_1 q_1^2 + 6 q_1^2 q_1) \\ = \varepsilon^2 \alpha_2 q_1^3 + \varepsilon^2 g_1 \cos(\tilde{\omega}^* t^*)\,,\end{aligned} \tag{15}$$

where $\omega_1 \approx 3.516$ is the fundamental linear frequency of a cantilevered beam. λ, α_1 and α_2 are numerical parameters obtained simply by algebraic operations and are completely related to the normalized mode functions.

$$\lambda \equiv \int_0^1 \phi_1 \phi_1 dx^* = 0.8582656856\,, \tag{16}$$

$$\beta_{11} \equiv \int_0^1 \phi_1 {\phi''}_1^3 dx^* = 7.406496639\,, \tag{17a}$$

$$\beta_{12} \equiv \int_0^1 \phi_1 {\phi'}_1^2 {\phi''}_1 dx^* = 4.310385928\,, \tag{17b}$$

$$\begin{aligned}\alpha_1 &\equiv 3a_3(D/L)^2\beta_{11} + r\beta_{12} \\ &\approx 3a_3(D/L)^2 \times 7.406496639 + r \times 4.310385928 \\ &\approx 38995.20480(D/L)^2 + 6.46557882\,,\end{aligned} \tag{18}$$

$$\beta_{21} \equiv \int_0^1 \phi_1[2\phi_1''(\phi_1''')^2 + (\phi_1'')^2\phi_1'''']dx^* = 119.6460118, \tag{19a}$$

$$\beta_{22} \equiv \int_0^1 \phi_1[2(\phi_1'')^2 + 6\phi_1'\phi_1''\phi_1''' + (\phi_1')^2\phi_1'''']dx^* = 20.21966456, \tag{19b}$$

$$\begin{aligned}\alpha_2 &\equiv 3a_3(D/L)^2\beta_{21} + r\beta_{22} \approx 3a_3(D/L)^2 \times 119.6460118 + r \times 20.21966456 \\ &\approx 6.299362521 \times 10^5 (D/L)^2 + 30.32949684\,.\end{aligned} \tag{20}$$

β_{11}, β_{12}, β_{21}, and β_{22} are also defined to simplify the calculation of α_1 and α_2.

Moreover, the nonlinear frequency $\tilde{\omega}^*$ can be expressed by perturbation parameter ε_1 as

$$\tilde{\omega}^* = \frac{\omega_1}{\sqrt{1-\lambda e_n^2}} - \sigma\varepsilon_1. \tag{21}$$

The solution for Eq. (15) and dimensionless excitation force can be, respectively, stated as

$$q_1(t^*, \varepsilon) = q_{10}(T_0, T_1) + \varepsilon_1 q_{11}(T_0, T_1) + \cdots \tag{22a}$$

$$\varepsilon^2 g_1 \cos(\tilde{\omega}^* t^*) = \varepsilon_1^2 g_1 \cos\left(\frac{\omega_1}{\sqrt{1-\lambda e_n^2}} T_0 - \sigma T_1\right), \tag{22b}$$

where

$$\varepsilon_1 = \varepsilon^2\,, \quad g_1 = \frac{G_1}{\varepsilon^3} \quad \text{and} \quad \upsilon = \frac{\mu}{\varepsilon^2}\,. \tag{22c}$$

T_0 and T_1 are slow and fast time scales due to the perturbation method of multiscales.[15]

Substituting Eqs. (22) into Eq. (15), and comparing the coefficients of the identical power of ε_1, we have

$$(\varepsilon_1^0) : (1-\lambda e_n^2) D_0^2 q_{10} + \omega_1^2 q_{10} = 0\,, \tag{23a}$$

$$\begin{aligned}(\varepsilon_1^1) : (1-\lambda e_n^2) D_0^2 q_{11} + \omega_1^2 q_{11} &= -2(1-\lambda e_n^2) D_0 D_1 q_{10} - 2\upsilon D_0 q_{10} + \alpha_2 q_{10}^3 \\ &- 6e_n^2 \alpha_1 (D_0 q_{10})^2 q_{10} - 3\mathrm{e}_n^2 \alpha_1 (D_0^2 q_{11}) q_{10}^2 + g_1 \cos\left(\frac{\omega_1}{\sqrt{1-\lambda e_n^2}} T_0 - \sigma T_1\right),\end{aligned} \tag{23b}$$

where $D_n = \partial/\partial T_n (n = 0, 1)$.

The generating solution can be obtained from Eq. (23a).

$$q_{10} = A(T_1) e^{i\frac{\omega_1}{\sqrt{1-\lambda e_n^2}}T_0} + \bar{A}(T_1) e^{-i\frac{\omega_1}{\sqrt{1-\lambda e_n^2}}T_0}. \tag{24}$$

Substituting q_{10} into Eq. (23b) gives

$$(1-\lambda e_n^2)D_0^2 q_{11} + \omega_1^2 q_{11} + 6e_n^2\alpha_1 D_0^2 q_{11} A(T1)\bar{A}(T1)$$
$$= -2\left[(1-\lambda e_n^2)\left(\frac{d}{dT_1}A(T_1)\right) + \upsilon A(T_1)\right]$$
$$\times\, i\frac{\omega_1}{\sqrt{1-\lambda e_n^2}} + 3\alpha_2 A(T1)^2\bar{A}(T1)$$
$$- 6e_n^2\alpha_1 A(T1)^2\bar{A}(T1)$$
$$\times\, \frac{\omega_1^2}{1-\lambda e_n^2} + \frac{g_1}{2e^{i\sigma T_1}} e^{i\frac{\omega_1}{\sqrt{1-\lambda e_n^2}}T_0}$$
$$- 3e_n^2\alpha_1 D_0^2 q_{11} A(T1)^2 e^{2i\frac{\omega_1}{\sqrt{1-\lambda e_n^2}}T_0}$$
$$+ \left(\alpha_2 A(T1)^3 + 6e_n^2\alpha_1 A(T1)^3\frac{\omega_1^2}{1-\lambda e_n^2}\right)$$
$$\times\, e^{3i\frac{\omega_1}{\sqrt{1-\lambda e_n^2}}T_0} + \mathrm{cc}, \tag{25}$$

where cc stands for the complex conjugate of preceding terms. Secular terms will be eliminated from the particular solution of Eq. (25) if we choose $A(T1)$ to be a solution of

$$-2\left[(1-\lambda e_n^2)\left(\frac{d}{dT_1}A(T_1)\right)\right] + \upsilon A(T_1)i\frac{\omega_1}{\sqrt{1-\lambda e_n^2}}$$
$$+ 3\alpha_2 A(T1)^2\bar{A}(T1) - 6e_n^2\alpha_1 A(T1)^2\bar{A}(T1)$$
$$\times\frac{\omega_1^2}{1-\lambda e_n^2} + \frac{g_1}{2e^{i\sigma T_1}} = 0\,. \tag{26}$$

To solve Eq. (26), we write A in the polar form

$$A(T_1) = \frac{1}{2}a(T_1)\exp(i\beta(T_1))\,, \tag{27}$$

where a and β are real functions of the slow time scale T_1. Then by separating the result into its real and imaginary parts, we obtain

$$8\omega_1(1-\lambda e_n^2)^2 a'$$
$$= -8\upsilon\omega_1(1-\lambda e_n^2)a$$
$$+ 4g_1(-1+\lambda e_n^2)^{\frac{3}{2}}\sin(\beta(T_1)+\sigma T_1)$$
$$- 8\omega_1(1-\lambda e_n^2)^{\frac{3}{2}}a\beta'$$
$$= -(3\alpha_2\lambda e_n^2 - 3\alpha_2 + 6e_n^2\alpha_1\omega_1^2)a^3$$
$$+ 4g_1(1-\lambda e_n^2)\cos(\beta(T_1)+\sigma T_1)\,. \tag{28}$$

For the steady-state response in the neighborhood of singular points, every small perturbation motion has to decay and this occurs when $a' = \beta' = 0.$[13] Therefore,

$$8\upsilon\omega_1\sqrt{1-\lambda e_n^2}a = -4g_1(1-\lambda e_n^2)\sin(\gamma)\,,$$
$$8\omega_1(1-\lambda e_n^2)^{\frac{3}{2}}a\sigma + (3\alpha_2\lambda e_n^2 - 3\alpha_2 + 6e_n^2\alpha_1\omega_1^2)a^3$$
$$= 4g_1(1-\lambda e_n^2)\cos(\gamma)\,, \tag{29}$$

where $\gamma = \beta(T_1) + \sigma T_1$.

By omitting γ from Eqs. (29), it can be written as

$$64\upsilon^2\omega_1^2(1-\lambda e_n^2)a^2 + [8\omega_1(1-\lambda e_n^2)^{\frac{3}{2}}\sigma$$
$$+ (3\alpha_2\lambda e_n^2 - 3\alpha_2 + 6e_n^2\alpha_1\omega_1^2)a^2]^2a^2$$
$$= 16g_1^2(1-\lambda e_n^2)^2\,. \tag{30}$$

The solution of the nonlinear Eq. (15) is given by

$$q_1 = a\cos\left(\frac{\omega_1}{\sqrt{1-\lambda e_n^2}}t^* + \beta\right) + O(\varepsilon)\,. \tag{31}$$

and the maximum vibration amplitude is expressed as

$$a = \frac{\sqrt{1-\lambda e_n^2}g_1}{2\omega_1\upsilon} \tag{32}$$

and

$$\beta = \gamma - \sigma T_1. \tag{33}$$

In Eq. (33), σ represents a variable of maximum vibration amplitude a, and is written as

$$\sigma = -\frac{3}{32}\frac{g_1^2(\alpha_2\lambda e_n^2 - \alpha_2 + 2\alpha_1 e_n^2\omega_1^2)}{\upsilon^2\omega_1^3\sqrt{1-\lambda e_n^2}}\,. \tag{34}$$

Eventually, by using Eq. (21), the nonlinear resonance frequency of the CNT due to the rippling effect can be determined.

$$\tilde{\omega}^* = \frac{\omega_1}{\sqrt{1-\lambda e_n^2}} - \sigma\varepsilon_1$$
$$= \frac{\omega_1}{\sqrt{1-\lambda e_n^2}}$$
$$+ \frac{3}{32}\frac{g_1^2(\alpha_2\lambda e_n^2 - \alpha_2 + 2\alpha_1 e_n^2\omega_1^2)}{\upsilon^2\omega_1^3\sqrt{1-\lambda e_n^2}}\varepsilon_1\,. \tag{35}$$

Using Eq. (22c), the final form of nonlinear resonant frequency will be

$$\tilde{\omega}^* = \frac{\omega_1}{\sqrt{1-\lambda e_n^2}}$$
$$+ \frac{3}{32}\frac{G_1^2(\alpha_2\lambda e_n^2 - \alpha_2 + 2\alpha_1 e_n^2\omega_1^2)}{\mu^2\omega_1^3\sqrt{1-\lambda e_n^2}}\,. \tag{36}$$

From Eq. (27) in Ref. 11, we have

$$\frac{E_{\text{eff}}}{E} = \left(\frac{\tilde{\omega}}{\bar{\omega}}\right)^2 = \left(\frac{\tilde{\omega}^*}{\bar{\omega}^*}\right)^2, \tag{37}$$

where $\bar{\omega}^*$ is defined as

$$\bar{\omega}^* = \frac{\omega_1}{\sqrt{1-\lambda e_n^2}} \tag{38}$$

and E represents Young's modulus of SWCNT without rippling deformation.

Thus, by substituting Eqs. (36) and (38) into Eq. (37), the effective bending modulus due to the rippling deformation E_{eff} can be calculated as

$$\frac{E_{\text{eff}}}{E} = \left(1 + \frac{3}{32}\,\frac{G_1^2\left(\alpha_2\lambda e_n^2 - \alpha_2 + 2\alpha_1 e_n^2\omega_1^2\right)}{\mu^2\omega_1^4}\right)^2. \tag{39}$$

Equation (39) indicates that the effective Young's modulus E_{eff} of a SWCNT with rippling deformation is a function of the dimensionless nonlocal parameter ($e_n = e_0a/L$), the excitation load-to-damping ratio (G_1/μ), and the diameter-to-length ratio (D/L).

Furthermore, the rippling deformation may cause the model to experience structural instability, especially in large deformations, as the effective bending modulus-to-Young's modulus ratio (the effective bending modulus ratio) E_{eff}/E reduces to zero.

3. Results and Discussion

In this study, the governing equation of motion of a cantilevered SWCNT with rippling deformation has been derived using nonlocal Euler–Bernoulli beam theory. It is assumed that the CNT has been oscillated in a harmonic electrical field for predicting the effective Young's modulus and the conditions in which the structural instability due to rippling deformation occurs.

Based on the nonlocal elastic theory, our model shows that there are three important factors that influence the effective bending modulus of CNTs with rippling deformation: (1) the dimensions of SWCNT; (2) the amplitude of the exerted harmonic force; and (3) the nonlocal parameter (see Eq. (39)).

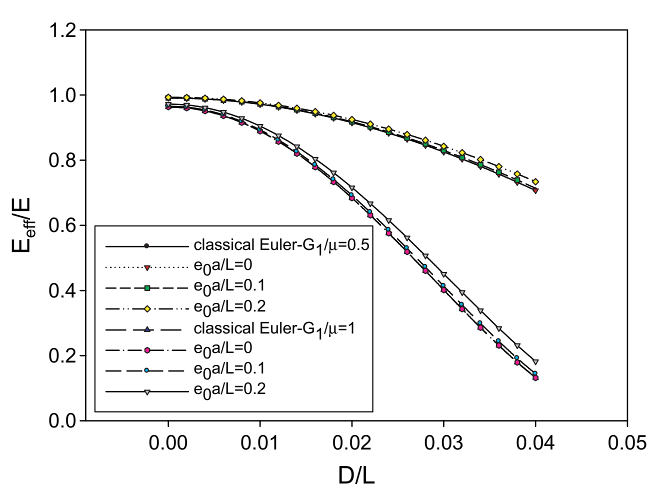

Fig. 1. The corresponding relation between E_{eff}/E and D/L with different G_1/μ and e_0a/L.

Figure 1 shows the effective bending modulus ratio E_{eff}/E as a function of dimensionless D/L for the cantilevered SWCNT with different dimensionless nonlocal parameters e_0a/L and two different excitation load-to-damping ratios G_1/μ. If the dimensionless nonlocal ratio is equal to zero ($e_n = e_0a/L = 0$), the results will be for the classical Euler–Bernoulli beam theory and exactly the same as in Ref. 11. The figure demonstrates that the effective bending modulus of a CNT with the rippling deformation decreases as the dimensionless D/L and excitation load-to-damping ratio G_1/μ increase. Moreover, the nonlinear nonlocal model predicts larger values for effective bending modulus with rippling deformations relative to the classical Euler–Bernoulli beam theory, especially for huge values of excitation load-to-damping ratio G_1/μ and dimensionless D/L. For instance, the classical Euler–Bernoulli beam theory predicts an effective bending modulus for a cantilevered CNT with D/L equal to 0.035, of about 1 Tpa without rippling deformation and about 0.25 Tpa due to the rippling deformation while this model estimates it about 0.311 Tpa when $e_0a/L = 0.2$, $G/\mu = 1$.

As mentioned before, the rippling phenomenon may cause CNTs to experience a special kind of structural instability called rippling instability especially for large bending displacements. Under certain conditions, the high stiffness in addition to the high flexibility of CNTs cause ripple configurations to appear in the internal radius of a bent CNT that can reduce the effective bending modulus down to zero, and consequently Eq. (39) can predict the conditions for which the rippling instability should occur.

Figure 2 shows the parameters' influence on the rippling instability threshold (i.e., $E_{\text{eff}}/E = 0$) for a cantilevered SWCNT. The dimensionless nonlocal ratio e_0a/L, the excitation load-to-damping ratio G_1/μ, and the diameter-to-length ratio D/L are

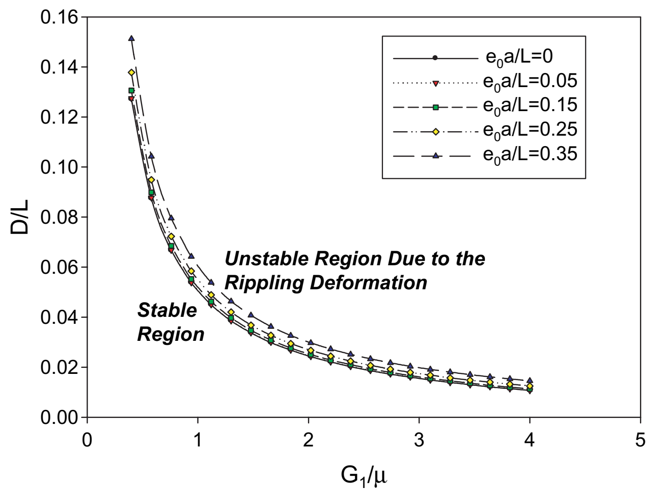

Fig. 2. The load-to-damping ratio G_1/μ against the diameter-to-length ratio with different values of dimensionless nonlocal parameter e_0a/L for the rippling instability threshold.

the parameters. It is seen from the figure that as the excitation load-to-damping ratio G_1/μ increases the rippling instability threshold occurs in a smaller diameter-to-length ratio D/L. Meanwhile, the results indicate that the rippling instability occurs for CNTs with higher values of D/L as the dimensionless nonlocal ratio e_0a/L increases.

4. Conclusions

Based on the nonlocal Euler−Bernoulli beam theory, the nonlinear vibrational model for cantilevered SWCNTs with the rippling deformation has been developed. The nonlinear resonant frequency and the associated effective bending modulus of a bent CNT have been obtained using the perturbation method of multiscales. The results indicate that the rippling deformation causes the effective bending modulus decrease dramatically for the short CNTs, especially for the high exciting harmonic force. Furthermore, the nonlocal theory predicts the higher values for the effective bending modulus with respect to the classical Euler−Bernoulli beam theory for stubby CNTs. The threshold of the rippling instability and the parameters' influence on it are also discussed widely, and the results point out that the nonlocal model predicts rippling instability for the CNTs with higher values of diameter-to-length compared with the classical Euler−Bernoulli beam theory.

References

1. S. Iijima, *Nature* **354**, 56 (1991).
2. M. S. Dresselhaus, G. Dresselhaus and P. H. Avouris, *Topics. Appl. Phys.* **80**, 287 (2001).
3. P. H. Avouris, T. Hertel, R. Martel, T. Schmidt, H. R. Shea and R. E. Walkup, *Appl. Surf. Sci.* **141**, 201 (1999).
4. W. Yang, X. L. Ma, H. T. Wang and W. Hong, *Adv. Mech.* **32**, 161 (2002).
5. Yu. E. Lozovik, A. V. Minogin and A. M. Popov, *Phys. Lett. A* **313**, 112 (2003).
6. M. M. J. Treacy, T. W. Ebbesen and J. M. Gibson, *Nature* **38**, 678 (1996).
7. A. Krishnan, E. Dujardin, T. W. Ebbesen *et al.*, *Phys. Rev. B* **58**, 14013 (1998).
8. E. W. Wong, P. E. Sheehan and C. M. Liebert, *Science* **277**, 1971 (1997).
9. P. Poncharal, Z. L. Wang, D. Ugarte and W. A. de Heer, *Science* **283**, 1513 (1999).
10. J. Z. Liu, Q. Zheng and Q. Jiang, *Phys. Rev. Lett.* **86**, 4843 (2001) Doi: 10.1103.
11. X. Wang, X. Y. Wang and J. Xiao, *Compos. Struct.* **69**, 315 (2005).
12. Y. Yan, W. Q. Wang and L. X. Zhang, *Mod. Phys. Lett. B* **22**, 2769 (2008).
13. J. Peddieson, G. R. Buchanan and R. P. McNitt, *Int. J. Eng. Sci.* **41**, 305 (2003).
14. P. Lu, H. P. Lee, C. Lu and P. Q. Zhang, *Int. J. Solids Struct.* **44**, 5289 (2007).
15. A. H. Nayfeh and D. T. Mook, *Nonlinear Oscillations* (Wiley, New York, 1997).